Journal of Materials Chemistry C

ROYAL SOCIETY OF CHEMISTRY

PERSPECTIVE

View Article Online
View Journal | View Issue

Cite this: J. Mater. Chem. C, 2023, 11, 16117

Bridging the gap from single molecule properties to organic semiconductor materials

Qian Zhan,[a] Dacheng Dai,[a] Fang Miao,[bc] Dongsheng Wang, *[a] Xiaodong Liu *[a] and Yonghao Zheng *[ab]

Received 13th July 2023,
Accepted 17th October 2023

DOI: 10.1039/d3tc02462h

rsc.li/materials-c

Organic semiconductors (OSCs), as a kind of plastic electronic material that can be prepared at low cost and on large areas, have great potential for applications in organic light-emitting diodes, organic field-effect transistors, organic photovoltaics, organic photodetectors, and organic thermoelectrics. In this burgeoning field, it is becoming very important to design OSCs in a more efficient manner. Unlike current characterization methods, single-molecule junctions allow a deeper exploration of the intrinsic charge transport properties inside a molecule. In this perspective, we will discuss how single-molecule characterization techniques can help to establish structure–property relationships and further open up new paths for the rational design of OSC materials.

1. Introduction

In 1977, the discovery of conducting *trans*-polyacetylene by Shirakawa *et al.*[1] sparked great interest in the field of organic semiconductors (OSCs), which have become one of the most exciting interdisciplinary research fields from chemistry, physics, engineering to biology. Because of their excellent electronic properties, solution processability, flexibility, and low fabrication cost, OSC materials have been used in the development of advanced electronic devices such as organic light-emitting diodes (OLEDs),[2–5] organic field-effect transistors (OFETs),[6–8] organic photovoltaics (OPVs),[9–12] organic photodetectors (OPDs),[13–16] and organic thermoelectrics (OTEs).[17–20]

Given that OSCs exhibit chemical and structural diversity at the molecular level, it requires a great deal of effort and dedication from researchers to establish clear structure–property relationships on the basis of a large number of complex systems. The design and development of high-performance OSCs can be better facilitated if molecular structures and properties of OSC materials can be precisely linked.

Molecular-scale electronics is widely investigated in depth as a hotspot because it not only meets the technical requirements for the increasing miniaturization of conventional silicon-based electronic devices but also provides an ideal platform to explore the intrinsic properties of materials at the molecular level.[21,22] The optical, electrical, magnetic, and stacking properties of molecular junctions can be characterized by using single-molecule techniques. Conventional techniques for OSC characterization only give an overall result of the bulk materials. In contrast, single-molecule techniques principally provide a solution to detect individual molecules and thus can exclude this average effect. We can discover new phenomena and uncover the basic laws hidden in conventional ensemble-average measurements. It is important to emphasize that, unlike conventional material characterization, single-molecule junction experiments may provide a fundamental understanding of the intrinsic electronic structure and continuously help us to clarify structure–function relationships and design principles at the molecular scale. To date, three major classes of molecular junction fabrication methods have been developed (Fig. 1).[23]

This perspective aims to introduce single-molecule characterization techniques to promote the development of OSC materials, which opens up a new perspective different from the existing methods and thereby can accelerate the molecular design for advanced organic electronic materials.

[a] School of Optoelectronic Science and Engineering, University of Electronic Science and Technology of China (UESTC), Chengdu 610054, People's Republic of China. E-mail: zhengyonghao@uestc.edu.cn, xdliu@uestc.edu.cn, wangds@uestc.edu.cn
[b] State Key Laboratory of Organic Electronics and Information Displays & Institute of Advanced Materials (IAM), Nanjing University of Posts & Telecommunications, 9 Wenyuan Road, Nanjing 210023, People's Republic of China
[c] Institute of Electronic and Information Engineering of UESTC in Guangdong, Zongbu Second Road No. 17, Dongguan, Guangdong 523808, People's Republic of China

2. Single-molecule electroluminescence

Scanning tunneling microscopy induced luminescence (STML) is a technique that utilizes highly localized tunneling electrons as an excitation source for emitting photons, providing unprecedented opportunities to gain insight into the radiative

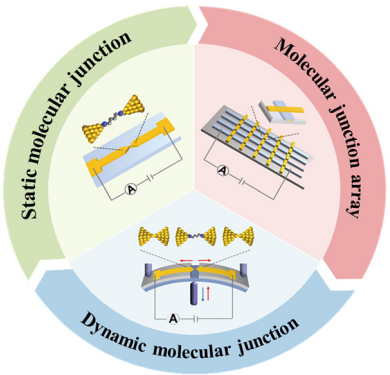

Fig. 1 Fabrication of molecular junctions. Reproduced with permission.[23] Copyright 2022, Institute of Physics Publishing.

properties of molecules at a single-molecule level.[24–27] Using a scanning tunneling microscope (STM), Kimura *et al.*[27] reported a 3,4,9,10-perylenetetracarboxylicdianhydride (PTCDA) molecule, which was adsorbed on a three-monolayer-thick NaCl film atop Ag(111) (Fig. 2(a)). Both phosphorescence and fluorescence signals were observed at high applied voltage (Fig. 2(b)). The STML spectrum shows two main peaks at 2.45 eV (506 nm) and 1.33 eV (932 nm), which can be assigned to the 0–0 transition of fluorescence and 0–0 transition of phosphorescence, respectively. This assignment is based on previous photoluminescence results, time-dependent density functional theory calculations, and the peak widths of the 0–0 transitions (Fig. 2(d)). In contrast to the high-bias luminescence spectrum, only phosphorescence appears at low applied voltage, demonstrating the selective formation of spin-triplet (T_1) excitons without producing their spin-singlet (S_1) counterparts. It should be mentioned that this is the first observation of phosphorescence from PTCDA, and also the first observation of phosphorescence in a single-molecule STML measurement. To reveal the mechanism of the selective T_1 formation, the voltage dependence of the STML spectra was examined, in combination with a dI_t/dV_s measurement in the negative sample voltage region. The removal of the 'anti-parallel' electron from the highest occupied molecular orbital (HOMO) of the −1 charged state is the primary mechanism of T_1 formation (Fig. 2(e)). This work offers a simple way to achieve the selective and direct formation of T_1 excitons at low applied voltages. In addition to charged molecules, radical molecules, which also have an unpaired electron, could be suitable for implementing selective T_1 formation in OLEDs. Designing a device taking into account the exchange interaction could realize an OLED with a lower operating voltage. A STM combined with optical detection systems provides atomically accurate spectroscopy for studying the optical and electron-transport processes, elucidates the fundamental exciton physics in well-defined molecular systems, and creates the basis for the design of emitters at the single-molecule and quantum levels.

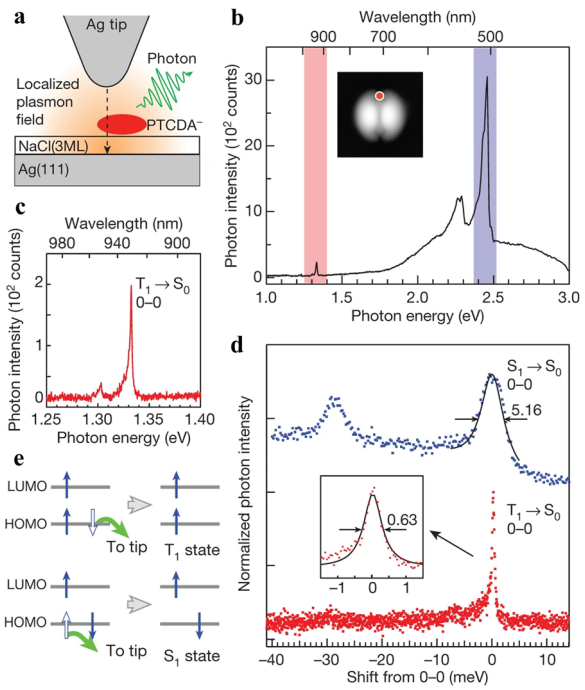

Fig. 2 STML fluorescence and phosphorescence spectra of the PTCDA/NaCl(3ML)/Ag(111) system. (a) Schematic of the STML measurement. (b) STML spectrum of a PTCDA molecule (V_s = −3.5 V) at a low energy resolution; see below for red and blue shaded regions. The tip position is shown as a red dot in the inset STM image. (c) STML spectra at a medium energy resolution and a photon energy of 1.25–1.40 eV (red region in b). (d) Peak widths of the 0–0 transitions of fluorescence (blue, V_s = −3.5 V) and phosphorescence (red, V_s = −2.5 V) at a high energy resolution. Black lines show Lorentzian fitting results. (e) Schematic images of the exciton formation mechanism; the blue arrows represent electrons. Reproduced with permission.[27] Copyright 2019, Springer Nature.

In 2010, Marquardt *et al.*[28] reported the observation of electroluminescence from a rod-like molecule that consists of a 2,6-dibenzylamino core-substituted naphthalenediimide (NDI) chromophore, two long oligo-phenylene ethynylene (OPE) rods, and phenanthrene anchor units. The organic molecule was accommodated between two metallic single-walled carbon nanotube electrodes. Electroluminescence starts to appear at voltages larger than 4 V. The collected electroluminescence spectrum of the nanotube–molecule–nanotube (NT–M–NT) junction coincided with the fluorescence spectrum of the rod-like molecules deposited on a highly ordered pyrolytic graphite (HOPG) surface in terms of peak position, width and overall spectral shape. Thus, electroluminescence of the molecule can be turned on and off by controlling the voltage bias, which opens up new possibility for achieving single-molecule junction electroluminescence at room temperature. Schull *et al.*[29] used the tip of a STM to controllably lift a thiophene molecular wire from the Au(111) surface. Under a forward bias, electroluminescence occurred at the wire junction, stemming from the recombination of electrons injected from the tip in the lowest unoccupied molecular orbital (LUMO) with holes injected from the sample in the HOMO of the molecular wire. When the thiophene units were detached from the surface, it led to conformational changes of the wires, affecting the electron delocalization length and the emission wavelength. For the opposite polarity, an emission was strongly

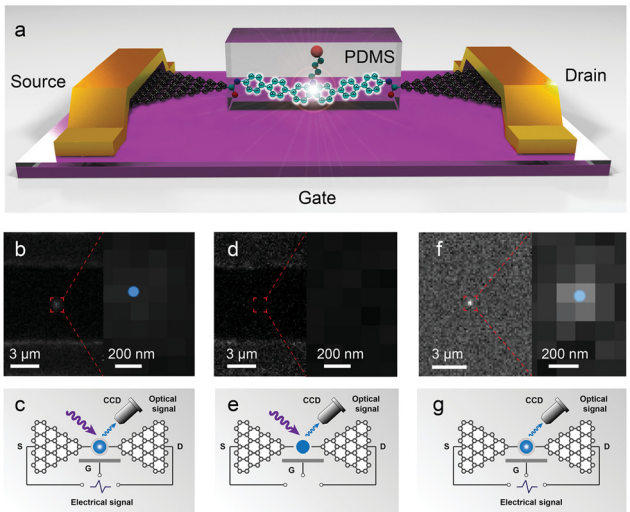

Fig. 3 Schematic illustration and imaging of an SM-LED. (a) Schematic representation of the device. (b) and (c) Superhigh-resolution image of an SM-LED by stochastic optical reconstruction microscopy and the corresponding experimental setup. (d) and (e) Superhigh-resolution image of the same SM-LED without the electric input, showing no obvious light spot, and the corresponding experimental setup. (f) and (g) Superhigh-resolution image of the same SM-LED without the excited light and the corresponding experimental setup. Reproduced with permission.[30] Copyright 2023, John Wiley and Sons.

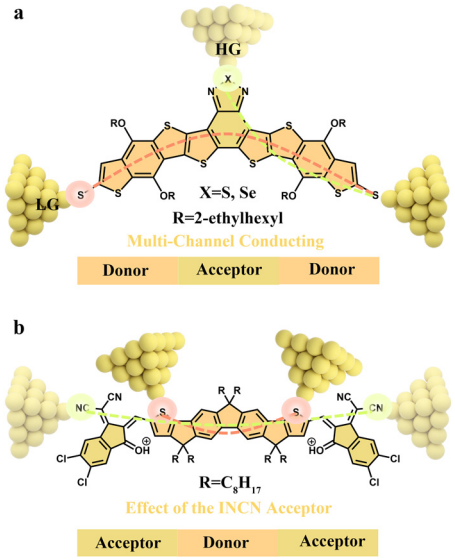

Fig. 4 (a) Multiple charge transfer pathways of donor–acceptor ladder-type molecules. Reproduced with permission.[31] (b) Schematic illustration of single-molecule junctions for the acceptor–donor–acceptor structure using different anchor groups. Effect of the INCN acceptor on the electronic characteristics of the donor center after molecule protonation. Reproduced with permission.[32]

attenuated. Both the polarity dependence and the emission mechanism are consistent with the behaviour of a single polymer light emitting diode. Recently, Guo's group[30] covalently integrated a carbazole-based molecule into graphene electrodes to prepare a robust single-molecule light-emitting diode (SM-LED) with high color purity, linear polarization, and efficient tunability. The superhigh-resolution image shows only one bright spot that strongly demonstrates the single-molecule connection. The optical signal originates from electroluminescence, which is confirmed by performing comparison experiments without electric inputs or excited light, ruling out the possibility of photoluminescence (Fig. 3). A single-photon counter was further introduced to the photoelectrical integration system with high temporal/spatial/energy resolution to characterize the single-photon emission of the SM-LED. Additionally, rational molecular engineering enables the fabrication of a multicolor SM-LED by achieving single-molecule Förster resonance energy transfer from the electroluminescent center to various acceptors. Overall, single-molecule junctions offer a new opportunity to deeply understand the electronic structure and luminescence mechanism at the molecular level.

3. Single-molecule conductance characteristics

Organic donor–acceptor molecules, used as active layers across extraordinary charge pathways, facilitate charge separation and transport in OFETs and OPVs. Yu's group[31] synthesized a series of donor–acceptor ladder-type molecules and investigated their multiple-charge transfer pathways using the STM-based break-junction (STM-BJ) technique. The high-conductance pathway is identified as the transmission through one thiol group and the central benzodiazole group, whereas the low-conductance pathway arises from the transmission through the thiol groups (Fig. 4(a)). In addition, it is essential to investigate molecular electronic characteristics at the single-molecule level, particularly the function of bilateral acceptor groups, because the electronic properties of acceptor–donor–acceptor type molecules control light absorption, exciton separation, and charge transportation in the photovoltaic process. Recently, Li *et al.*[32] explored the electronic characteristics of acceptor–donor–acceptor type molecules by single-molecule charge transport. Specifically, it is discovered that the acceptor–donor–acceptor type molecules have higher conductance than the donor molecules with a shorter molecular length. This nonclassical high conductance is due to the additional transport channels contributed by the 1,1-dicyano methylene-3-indanone (INCN) acceptor units. Furthermore, protonation opens the S···O noncovalent conformational lock, exposing the –S anchoring sites and enabling the direct detection of charge transport of the donor central part, which further confirms that the conductive orbitals contributed by the INCN acceptor groups could penetrate the whole acceptor–donor–acceptor molecule (Fig. 4(b)). These results provide important insights into the development of high-performance materials for organic solar cells.

The length, the number, and the substitution position of alkyl side chains incorporated into organic conjugated molecules have large effects on their charge transport properties. Schroeder's group[33] studied the conductance properties of a

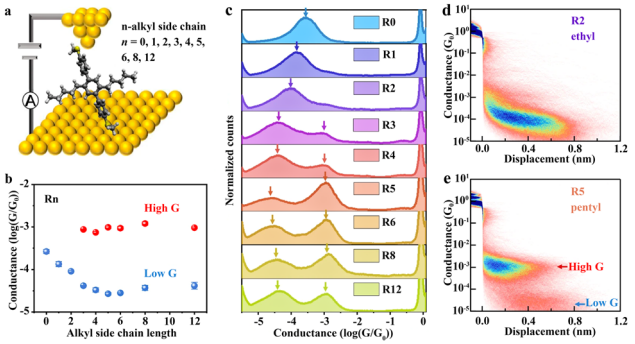

Fig. 5 Single-molecule characterization of charge transport in terphenyl derivatives with different alkyl side chains. (a) Schematic of the Au–Rn–Au junction. (b) Conductance peak values of 1 mM Rn at 0.25 V applied bias. (c) 1D conductance histograms of 1 mM Rn at 0.25 V bias voltage, each constructed from >4000 traces. (d) and (e) Representative 2D conductance histograms of R2 and R5. Reproduced with permission.[33] Copyright 2022, Springer Nature.

library of symmetric terphenyl derivatives with different alkyl side chains (Rn) using a STM-BJ (Fig. 5). Interestingly, these terphenyl derivatives exhibit an unexpected dependence of molecular conductance on the alkyl chain length. Particularly, R0–R2 only shows a single distinct conductance peak, and molecular conductance drops with an increase in alkyl chain length. In contrast, R3–R12 presents two dominant and well-spaced conductance states (high G and low G). Interestingly, the conductance of the high G state is independent of the alkyl side chain length, and the value is more than one order of magnitude larger than the low G state. Here, the high G state corresponds to a molecular conformation in which the molecule is "lying down" on the electrode surface *via* side chain-mediated van der Waals interactions, whereas the low G state corresponds to a "standing up" upright molecular conformation with a junction anchored at both termini to metal electrodes. Furthermore, the concentration-dependent conductance behaviour of the high G state suggests that the "lying down" conformation becomes increasingly dominant as the solution concentration increases. This work deepens our understanding of structure–property relationships in OSC materials and emphasizes the need to fully understand the impact of side chain chemistry on charge transport. Manipulation of the molecular conformation using different side chain chemistries is useful for informing complementary studies on side chain engineering involving OSC materials and opens new avenues for understanding the electronic structure of materials.

4. Single-molecule magnetism characteristics

Recently, single-molecule junctions combined with various multimodal control systems have been extensively used to examine important physical phenomena due to their robust monitoring and control abilities. In this section, we focus on the potential applications of single-molecule techniques in the characterization and modulation of the spin properties of OSC magnetic materials.

The Kondo effect, which is caused by unpaired electrons in radicals[34–38] and metal complexes, can be utilized to determine whether a molecule contains spins in single-molecule devices.[39,40] In addition, the Kondo effect can be finely tuned by the Zeeman effect, which causes the splitting of the energy levels of spin electrons when a magnetic field is applied to the molecule. Specifically, the Zeeman effect could be observed in single-molecule transistors incorporating the molecules containing a Co^{2+} ion with spin electrons bonded to polypyridyl ligands.[40] The molecules are attached to insulating tethers of different lengths, serving as conductive channels. The zero-bias differential conductance dI/dV peak splits in the magnetic field and the splitting is enhanced with the increasing magnetic field.

The single-molecule junction enables the regulation of the spin state of the metal complexes. Usually, external stimuli such as electric fields,[41] mechanical manipulation,[42] and temperature[43] can be used to switch the low-spin (LS) and high-spin (HS) states of the molecule. For instance, Fe^{II} complexes are typical spin-crossover molecules in single-molecule junctions (Fig. 6(a)).[42] When the Fe atom is surrounded by an octahedral ligand environment (ligand field), its five spin-degenerate 3d levels split into a doublet and a triplet (Fig. 6(b)). The filling order of these levels with the six electrons of Fe^{II} depends on the ratio between the ligand field energy (E_{lf}) and the spin exchange energy (E_{exc}). If $E_{lf} \gg E_{exc}$, the electrons are all paired up, giving a total spin of $S = 0$, *i.e.*, the LS state. In the opposite case, $E_{exc} \gg E_{lf}$, the levels are filled according to Hund's rule and the spin is increased to a maximum value of $S = 2$, *i.e.*, the HS state. Specifically, in stretching-induced single-molecule switches, when the ligands are arranged perpendicularly, the complex is in the LS state. As the electrode spacing increases, the ligands are pulled further apart. The arrangement of two ligands is distorted, leading to a reduction of E_{lf}, which triggers the switch from the LS state to the HS state.

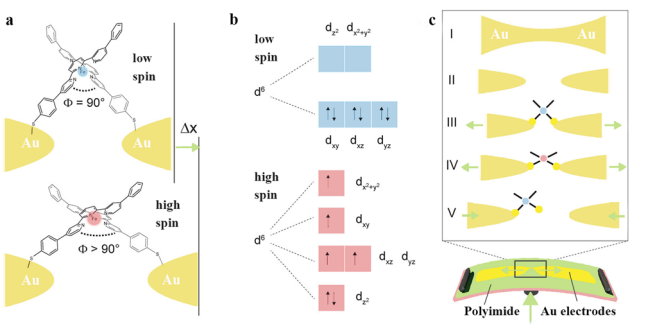

Fig. 6 Two-terminal mechanically controlled single-molecule junctions. (a) Sketch of the Fe^{II}-based spin-crossover molecular junction in the ideal arrangement to trigger the LS to HS switch by separating the electrodes by Δx. (b) Iron^{II} 3d levels involved in the spin-crossover phenomenon. (c) Schematic illustration of a mechanically controllable break junction (MCBJ) setup (bottom) with the molecule placed in the junction. Reproduced with permission.[42] Copyright 2016, American Chemical Society.

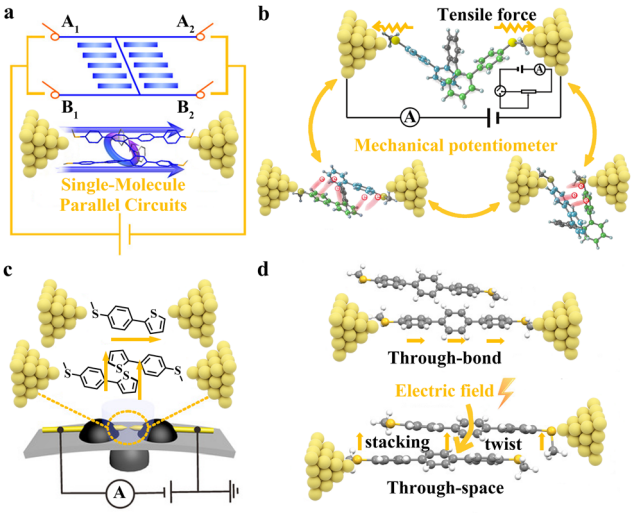

Fig. 7 (a) Illustration of the electron-transport mechanism and a controllable multichannel-molecular-device model based on the single-molecule parallel circuits. Reproduced with permission.[46] Copyright 2020, John Wiley and Sons. (b) Schematic illustration of a mechanical single-molecule potentiometer based on *ortho*-pentaphenylene foldamers. Reproduced with permission.[47] Copyright 2021, Springer Nature. (c) Illustration of the MCBJ technique with a single-molecule junction (top) and a single-stacking junction (bottom). Reproduced with permission.[49] Copyright 2019, John Wiley and Sons. (d) Schematic of single-molecule junctions and single-stacking junctions of terphenyl. Reproduced with permission.[55] Copyright 2020, American Chemical Society.

Using mechanically controllable gold nanoelectrodes, the zero-bias conductance can be monitored during stretching the electrodes, which displays a conductance increase when increasing the electrode separation and this increase can reach 1–2 orders of magnitude.

5. π–π stacking interactions

The macroscopic properties of OSCs are affected not only by the properties of individual molecules, but also by molecular stacking. It is essential to understand the relationships between molecular stacking features and their electrical properties at the molecular level, which facilitates further development of functional materials for applications in OFETs and OPVs.

Intramolecular π-stacking interactions can effectively improve the charge transport ability of molecules. Unlike the widely used planar conformations, folded single molecules have intramolecular π–π stacking interactions. Deciphering multichannel charge transport in single-molecule junctions using the STM-BJ technique provides a conceptual advancement in the single-molecule multichannel conductance (Fig. 7(a) and (b)).[44–47] Tang's group[47] designed and characterized a series of *ortho*-pentaphenylene derivatives with multiple folded conformers. These derivatives undergo conformational interconversion between antiparallelly folded structures and co-parallelly folded structures in solutions. Owing to conformational changes, multiple conductances were observed, with the high-conductance state originating from the co-parallelly folded conformer and the low-conductance state belonging to the antiparallelly folded conformer. In addition, the folded conformers are sensitive to solvents, leading to feasible conductance modulation. Although the highly twisted molecular backbones lead to weak through-bond conjugation, the antiparallelly folded conformers exhibit significantly higher conductance compared to the linear *para*-pentaphenylene isomers. This demonstrates the effective compensating conductance resulting from the through-space coupling between closely stacked aromatic rings. The flicker noise analysis provides further evidence for the coexistence of both the through-bond and through-space pathways for charge transport, which contributes to the remarkable characteristic of multichannel conductance. This not only enables high conductance but also aids in understanding the mechanism of charge transport in higher-order helical molecules. Furthermore, these pseudo-elastic folded molecules can be mechanically stretched and compressed by the force exerted using the Au tip, resulting in a dramatically variable conductance of up to two orders of magnitude.

Furthermore, exploring the mechanisms of intermolecular π-stacking interactions is of great importance for the design of multifunctional materials.[48–50] Hong's group[49] investigated the intramolecular and intermolecular charge transport properties in single-molecule and single-stacking thiophene junctions using the MCBJ technique (Fig. 7(c)). Intramolecular and intermolecular charge transports in thiophene junctions can be distinguished by flicker noise analysis. They surprisingly found that intermolecular rather than intramolecular charge transport may be the dominant charge transport path in OSC molecules with large conjugation. Specifically, the conductance of thiophene-based single-stacking junctions is nearly independent of the conjugation pattern, which contrasts with the notable length dependence of conductance in single-molecule junctions with the same building blocks. The dominant charge-transport path transits from an intramolecular path to an intermolecular path when the conjugated region increased. These findings provide a fundamental insight into how molecular aggregation increases the formation probability of intermolecular charge transport channels and thus enhances the charge transport through π-conjugated OSC materials.

6. Conclusions and perspectives

The potential of single-molecule techniques as a characterization tool allows a deeper exploration of the intrinsic charge transport mechanisms of materials and to provide fundamental insights into the electronic structure of building blocks in OSC materials. The single-molecule experimental measurements can be used to assess high-performance materials and to expand the range of material characterization strategies. Understanding and modulating the optical, electrical, magnetic, and stacking properties of single molecules contributes to a deeper understanding of structure–property relationships,

and these knowledge and information help in the design, development, and optimization of OSC materials.

Molecular engineering is likely to revolutionize the landscape of materials chemistry. Understanding the structure–property relationships at the single-molecule level is still an ongoing research topic that requires untiring efforts and collaboration between researchers from various disciplines. Past achievements and upcoming prospects may offer new perspectives on the theories, materials, and devices in the area of OSCs.

Perspective 1. (a) STML can reveal the dependency between the conformational structures, energy levels, and optical characteristics of individual molecules, which has the advantages of high local excitations, high spatial resolution and local plasmon excitation. However, the understanding of STML is still inadequate. It is necessary to clarify the dominant excitation mechanisms, the excitation conditions, the complicated radiative transition processes, and the fundamental selection rules. Progress in this research area has the potential to facilitate the development of new semiconductor molecular light sources with specific properties in the future. (b) A thorough knowledge of intrinsic photophysics requires the simultaneous characterization of high-resolution optical and electrical properties. Single-molecule technology shows great promise for the accurate detection of single photons. Although device engineering at the molecular level is a daunting task, further development of SM-LEDs will be driven by continuous optimization of molecular engineering designs and the application of more OSC light-emitting materials to this field. (c) How to break the efficiency bottleneck caused by exciton spin statistics is the key in determining internal quantum efficiency (IQE). For organic monoradicals, there is one unpaired electron in their highest singly occupied molecular orbital (SOMO), which gives rise to the doublet excited state and totally spin-allowed radiative transition. It is worth mentioning that light-emitting radical emitters have already achieved a maximum external quantum efficiency of 27% at 710 nm, which is the highest value reported for deep-red and infrared LEDs.[51] Based on this, it may be possible to realize radical-based SM-LEDs that cleverly combine both the electrical and optical measurement techniques to gain a deeper understanding of the underlying luminescence mechanisms. In addition, the spin properties of multiradicals could be modulated at the molecular level by circularly polarized light and magnetic fields, leading to transitions between different excited states, which provides a new perspective on the modulation of excited states.

Perspective 2. Organic donor–acceptor molecules and side chain modifications are important strategies for fine-tuning the conjugated structures of OSCs. Single-molecule charge transport analysis reveals the intrinsic electronic properties of these molecules. In particular, exploring the function of the donor or acceptor moiety in the molecules can provide insights into the design of the molecules with flexible tunability. In addition, the use of single-molecule conductance measurements to investigate the effect of side chain modifications on charge transport in π-conjugated molecules deepens our understanding of the structure–function relationship of OSC materials. This further reinforces the importance of substitution sites, side chain chemistry, backbone identity, and side chain functionalization on charge transport to aid in the design of new high-performance OSC materials.

Perspective 3. (a) In general, the use of single-molecule devices to monitor the physical processes of single molecules offers the infinite possibility of discovering fundamental physical laws at the single-molecule level. The in-depth exploration of spin effects such as the Kondo effect, the Zeeman effect, and the spin-crossover effect at the single-molecule level can continuously deepen the understanding of magnetic phenomena in OSCs and advance the development of fields such as spintronics and molecular magnetism. (b) Single-molecule junctions can be utilized to monitor spin-crossover phenomena induced by various external stimuli, wherein accompanying changes in the molecular geometry and electronic configuration exert significant effects on molecular conductance. By fine-tuning the single-molecule spin states, the performance and controllability of OSC materials can be improved, while new functional materials can be developed. For example, modulating the spin states and coupling processes of radicals can change the electronic structure and spin distribution, affecting their conductivity, magnetism, optics, and other key properties, thus controlling their functions.[52,53]

Perspective 4. (a) Single-molecule techniques provide an ideal model for exploring electron transport in various π-stacked molecular systems. The quantitative description of intermolecular charge transport from a single-molecule perspective could explain that the existing aggregation in the microscopic charge transport of highly disordered materials increases the chances of intermolecular charge transport channel formation. Furthermore, the design strategy to construct through-space conjugated folded conformations may reduce the recombination energy and expand the charge transfer integral, which is beneficial for exploring robust electron transport materials. (b) The charge transport efficiency through π-stacked molecules is controlled by the electronic coupling between neighboring molecules and thus depends in a complex way on the distance and the respective orientation of the π-system. Single-molecule experiments provide a direct way to probe the modulation of π–π stacking interactions at the nanoscale and help in establishing the structure–property relationships for π-stacked molecules. In general, π–π stacking could be regulated by chemical control, electric fields, and mechanical forces. In terms of chemical modulation, the intermolecular stacking is hindered by introducing bulky *tert*-butyl substituents on the phenyl rings of oligophenyleneethynylene, and π–π stacking interactions are significantly weakened.[54] Moreover, electric fields have been shown to be a new green and smart tool for promoting molecular assembly at the single-molecule level. With the help of the single-molecule junction technique, it is possible to apply an electric field of about 10^8 V m^{-1} to nanoscale junctions and investigate the electric field-induced assembly at the single-stacking level (Fig. 7(d)).[55] In addition to electric fields, mechanical forces can also be used to modulate the stacking model of dimers.

Specifically, as the tip moves away from the substrate, the electronic structure will be changed due to the relative displacement of two molecules within the dimer, modifying the degree of dimer stacking.[56]

Author contributions

Q. Zhan: conceptualisation, investigation, visualisation, writing – original draft, and writing – review and editing. D. Dai: conceptualisation, investigation, and writing – review and editing. F. Miao: writing – review and editing. Prof. D. Wang: conceptualisation and writing – review and editing. Prof. X. Liu: conceptualisation, supervision, and writing – review and editing. Prof. Y. Zheng: conceptualisation, funding acquisition, project administration, and writing – review and editing.

Conflicts of interest

There are no conflicts to declare.

Acknowledgements

The authors acknowledge financial support from the National Natural Science Foundation of China (22375029 and 52203134), the Open Research Fund of the Chengdu University of Traditional Chinese Medicine State Key Laboratory Southwestern Chinese Medicine Resources (SKLTCM2022014), the Intelligent Terminal Key Laboratory of Sichuan Province (SCITLAB-20012 and SCITLAB-20013), the Guangdong Basic and Applied Basic Research Foundation (2021A1515110431), and the Open Research Fund of State Key Laboratory of Organic Electronics and Information Displays.

References

1 H. Shirakawa, E. J. Louis, A. G. MacDiarmid, C. K. Chiang and A. J. Heeger, *J. Chem. Soc., Chem. Commun.*, 1977, 578–580.
2 M. A. Baldo, D. F. O'Brien, Y. You, A. Shoustikov, S. Sibley, M. E. Thompson and S. R. Forrest, *Nature*, 1998, **395**, 151–154.
3 Y. Sun, N. C. Giebink, H. Kanno, B. Ma, M. E. Thompson and S. R. Forrest, *Nature*, 2006, **440**, 908–912.
4 H. Uoyama, K. Goushi, K. Shizu, H. Nomura and C. Adachi, *Nature*, 2012, **492**, 234–238.
5 J. Song, H. Lee, E. G. Jeong, K. C. Choi and S. Yoo, *Adv. Mater.*, 2020, **32**, 1907539.
6 G. Horowitz, *Adv. Mater.*, 1998, **10**, 365–377.
7 C. D. Dimitrakopoulos and P. R. L. Malenfant, *Adv. Mater.*, 2002, **14**, 99–117.
8 H. Li, W. Shi, J. Song, H. J. Jang, J. Dailey, J. Yu and H. E. Katz, *Chem. Rev.*, 2019, **119**, 3–35.
9 G. Yu, J. Gao, J. C. Hummelen, F. Wudi and A. J. Heeger, *Science*, 1995, **270**, 1789–1791.
10 L. Meng, Y. Zhang, X. Wan, C. Li, X. Zhang, Y. Wang, X. Ke, Z. Xiao, L. Ding, R. Xia, H.-L. Yip, Y. Cao and Y. Chen, *Science*, 2018, **361**, 1094–1098.
11 M. Madhu, R. Ramakrishnan, V. Vijay and M. Hariharan, *Chem. Rev.*, 2021, **121**, 8234–8284.
12 X. Li, H. Wang, J. A. Schneider, Z. Wei, W.-Y. Lai, W. Huang, F. Wudl and Y. Zheng, *J. Mater. Chem. C*, 2017, **5**, 2781–2785.
13 D. Periyanagounder, T.-C. Wei, T.-Y. Li, C.-H. Lin, T. P. Gonçalves, H.-C. Fu, D.-S. Tsai, J.-J. Ke, H.-W. Kuo, K.-W. Huang, N. Lu, X. Fang and J.-H. He, *Adv. Mater.*, 2020, **32**, 2070015.
14 J. Chen, W. Zhang, L. Wang and G. Yu, *Adv. Mater.*, 2023, **35**, 2210772.
15 W. Wang, X. Miao, G. Cai, L. Ding, Y. Li, T. Li, Y. Zhu, L. Tao, Y. Jia, Y. Liang, X. Lu, Y. Fang, Y. Yi and Y. Lin, *Adv. Mater.*, 2022, **34**, 2201600.
16 X. Liu, Y. Lin, Y. Liao, J. Wu and Y. Zheng, *J. Mater. Chem. C*, 2018, **6**, 3499–3513.
17 Q. Zhang, Y. Sun, W. Xu and D. Zhu, *Adv. Mater.*, 2014, **26**, 6829–6851.
18 H. Wang and C. Yu, *Joule*, 2019, **3**, 53–80.
19 W. Zhao, J. Ding, Y. Zou, C. A. Di and D. Zhu, *Chem. Soc. Rev.*, 2020, **49**, 7210–7228.
20 D. Zhou, H. Zhang, H. Zheng, Z. Xu, H. Xu, H. Guo, P. Li, Y. Tong, B. Hu and L. Chen, *Small*, 2022, **18**, 2200679.
21 X. Yang, S. Hou, M. Su, Q. Zhan, H. Zhang, S. M. Quintero, X. Liu, J. Liu, W. Hong, J. Casado, Q. Wu, C. J. Lambert and Y. Zheng, *J. Phys. Chem. Lett.*, 2023, **14**, 4004–4010.
22 L. Ge, S. Hou, Y. Chen, Q. Wu, L. Long, X. Yang, Y. Ji, L. Lin, G. Xue, J. Liu, X. Liu, C. J. Lambert, W. Hong and Y. Zheng, *Chem. Sci.*, 2022, **13**, 9552–9559.
23 Y. Zhao, W. Liu, J. Zhao, Y. Wang, J. Zheng, J. Liu, W. Hong and Z.-Q. Tian, *Int. J. Extreme Manuf.*, 2022, **4**, 022003.
24 X. H. Qiu, G. V. Nazin and W. Ho, *Science*, 2003, **299**, 542–546.
25 Y. Zhang, Y. Luo, Y. Zhang, Y. J. Yu, Y. M. Kuang, L. Zhang, Q. S. Meng, Y. Luo, J. L. Yang, Z. C. Dong and J. G. Hou, *Nature*, 2016, **531**, 623–627.
26 Y. Zhang, Q. S. Meng, L. Zhang, Y. Luo, Y. J. Yu, B. Yang, Y. Zhang, R. Esteban, J. Aizpurua, Y. Luo, J. L. Yang, Z. C. Dong and J. G. Hou, *Nat. Commun.*, 2017, **8**, 15225.
27 K. Kimura, K. Miwa, H. Imada, M. Imai-Imada, S. Kawahara, J. Takeya, M. Kawai, M. Galperin and Y. Kim, *Nature*, 2019, **570**, 210–213.
28 C. W. Marquardt, S. Grunder, A. Blaszczyk, S. Dehm, F. Hennrich, H. V. Lohneysen, M. Mayor and R. Krupke, *Nat. Nanotechnol.*, 2010, **5**, 863–867.
29 G. Reecht, F. Scheurer, V. Speisser, Y. J. Dappe, F. Mathevet and G. Schull, *Phys. Rev. Lett.*, 2014, **112**, 047403.
30 C. Yang, Y. Guo, S. Zhou, Z. Liu, Z. Liu, D. Zhang and X. Guo, *Adv. Mater.*, 2023, **35**, 2209750.
31 Z. Cai, N. Zhang, M. A. Awais, A. S. Filatov and L. Yu, *Angew. Chem., Int. Ed.*, 2018, **57**, 6442–6448.
32 P. Li, W. Xiong, J. Wang, J. Hao, M. Li, B. Wang, Y. Chen, W. Si, H. Ren, G. Li, Y. Chen, J. Lu, H. Zhang, C. Jia and X. Guo, *Adv. Mater.*, 2023, **35**, 2301876.

33 S. Li, E. R. Jira, N. H. Angello, J. Li, H. Yu, J. S. Moore, Y. Diao, M. D. Burke and C. M. Schroeder, *Nat. Commun.*, 2022, **13**, 2102.
34 K. Wang, Q. Zhan, B. Han, S. M. Quintero, W. Huang, Y. Ji, F. Miao, H. Chen, J. Casado and Y. Zheng, *J. Mater. Chem. C*, 2022, **10**, 12724–12730.
35 Y. Zheng, M. S. Miao, G. Dantelle, N. D. Eisenmenger, G. Wu, I. Yavuz, M. L. Chabinyc, K. N. Houk and F. Wudl, *Adv. Mater.*, 2015, **27**, 1718–1723.
36 Y. Shen, G. Xue, Y. Dai, S. M. Quintero, H. Chen, D. Wang, F. Miao, F. Negri, Y. Zheng and J. Casado, *Nat. Commun.*, 2021, **12**, 6262.
37 Y. Ding, S. Maitra, C. Wang, S. Halder, R. Zheng, T. Barakat, S. Roy, L. H. Chen and B. L. Su, *Interdiscip. Mater.*, 2022, **1**, 213–255.
38 G. Xiao, H. Xu, C. Bai, M. Liu and Y. B. He, *Interdiscip. Mater.*, 2023, **2**, 609–634.
39 W. Liang, M. P. Shores, M. Bockrath, J. R. Long and H. Park, *Nature*, 2002, **417**, 725–729.
40 J. Park, A. N. Pasupathy, J. I. Goldsmith, C. Chang, Y. Yaish, J. R. Petta, M. Rinkoski, J. P. Sethna, H. D. Abruna, P. L. McEuen and D. C. Ralph, *Nature*, 2002, **417**, 722–725.
41 G. D. Harzmann, R. Frisenda, H. S. van der Zant and M. Mayor, *Angew. Chem., Int. Ed.*, 2015, **54**, 13425–13430.
42 R. Frisenda, G. D. Harzmann, J. A. Celis Gil, J. M. Thijssen, M. Mayor and H. S. van der Zant, *Nano Lett.*, 2016, **16**, 4733–4737.
43 E. Burzuri, A. Garcia-Fuente, V. Garcia-Suarez, K. Senthil Kumar, M. Ruben, J. Ferrer and H. S. J. van der Zant, *Nanoscale*, 2018, **10**, 7905–7911.
44 L. Chen, Y. H. Wang, B. He, H. Nie, R. Hu, F. Huang, A. Qin, X. S. Zhou, Z. Zhao and B. Z. Tang, *Angew. Chem., Int. Ed.*, 2015, **54**, 4231–4235.
45 S. T. Schneebeli, M. Kamenetska, Z. Cheng, R. Skouta, R. A. Friesner, L. Venkataraman and R. Breslow, *J. Am. Chem. Soc.*, 2011, **133**, 2136–2139.
46 P. Shen, M. Huang, J. Qian, J. Li, S. Ding, X. S. Zhou, B. Xu, Z. Zhao and B. Z. Tang, *Angew. Chem., Int. Ed.*, 2020, **59**, 4581–4588.
47 J. Li, P. Shen, S. Zhen, C. Tang, Y. Ye, D. Zhou, W. Hong, Z. Zhao and B. Z. Tang, *Nat. Commun.*, 2021, **12**, 167.
48 S. Wu, M. T. Gonzalez, R. Huber, S. Grunder, M. Mayor, C. Schonenberger and M. Calame, *Nat. Nanotechnol.*, 2008, **3**, 569–574.
49 X. Li, Q. Wu, J. Bai, S. Hou, W. Jiang, C. Tang, H. Song, X. Huang, J. Zheng, Y. Yang, J. Liu, Y. Hu, J. Shi, Z. Liu, C. J. Lambert, D. Zhang and W. Hong, *Angew. Chem., Int. Ed.*, 2020, **59**, 3280–3286.
50 A. Magyarkuti, O. Adak, A. Halbritter and L. Venkataraman, *Nanoscale*, 2018, **10**, 3362–3368.
51 X. Ai, E. W. Evans, S. Dong, A. J. Gillett, H. Guo, Y. Chen, T. J. H. Hele, R. H. Friend and F. Li, *Nature*, 2018, **563**, 536–540.
52 H. Phan, S. M. Benjamin, E. Steven, J. S. Brooks and M. Shatruk, *Angew. Chem., Int. Ed.*, 2015, **54**, 823–827.
53 A. Kawamura, J. Xie, J. N. Boyn, K. A. Jesse, A. J. McNeece, E. A. Hill, K. A. Collins, J. A. Valdez-Moreira, A. S. Filatov, J. W. Kurutz, D. A. Mazziotti and J. S. Anderson, *J. Am. Chem. Soc.*, 2020, **142**, 17670–17680.
54 S. Martín, I. Grace, M. R. Bryce, C. Wang, R. Jitchati, A. S. Batsanov, S. J. Higgins, C. J. Lambert and R. J. Nichols, *J. Am. Chem. Soc.*, 2010, **132**, 9157–9164.
55 Y. Tang, Y. Zhou, D. Zhou, Y. Chen, Z. Xiao, J. Shi, J. Liu and W. Hong, *J. Am. Chem. Soc.*, 2020, **142**, 19101–19109.
56 R. Frisenda, V. A. Janssen, F. C. Grozema, H. S. van der Zant and N. Renaud, *Nat. Chem.*, 2016, **8**, 1099–1104.

